Rare Metal Materials and Engineering
Volume 51, Issue 3, March 2022
Available online at www.rmme.ac.cn

Science Press

Cite this article as: Zheng Jingwu, Chen Yishun, Fu Yongcheng, et al. Corrosion-Resistant Nanocrystalline Cu Coating by Ultrasonic Electrodeposition in Cyanide-Free Electrolyte[J]. Rare Metal Materials and Engineering, 2022, 51(03): 827-834.

ARTICLE

Corrosion-Resistant Nanocrystalline Cu Coating by Ultrasonic Electrodeposition in Cyanide-Free Electrolyte

Zheng Jingwu[1], Chen Yishun[1], Fu Yongcheng[1,3], Zhang Shuan[1], Qiao Liang[1], Cai Wei[1], Tang Yiping[1], Yi Xiaofei[2], Chen Jingwu[2], Li Wangchang[1], Ying Yao[1], Yu Jing[1], Liu Youhao[2], Huang Xiulian[2], Che Shenglei[1]

[1] Research Center of Magnetic and Electronic Materials, College of Materials Science and Engineering, Zhejiang University of Technology, Hangzhou 310014, China; [2] State Key Laboratory of Rare Earth Permanent Magnet Materials, Earth-Panda Advance Magnetic Material Co., Ltd, Hefei 231500, China; [3] China Key System & Integrated Circuit Co., Ltd, Wuxi 214072, China

Abstract: The nanocrystalline Cu protective coating was obtained on the Nd-Fe-B magnet matrix in the cyanide-free electrolyte by the ultrasonic-assisted electrodeposition under high cathodic current density. The coating morphology, crystallite size, microhardness, and corrosion resistance of the Cu coatings were analyzed under different ultrasonic frequencies. Results show that with increasing the ultrasonic frequency, the effective cathodic current density of Cu electrodeposition in the complex electroplating solution system is increased remarkably, and the corresponding current efficiency is enhanced, thereby achieving the dense nanocrystalline Cu coating. Under the condition of the cathodic current density of 4.0 $A \cdot dm^{-2}$ and frequency of 40 kHz, the Cu coating with the crystallite of 18.8 nm in size can be obtained. The bonding strength between the Cu coating and sintered Nd-Fe-B matrix is improved via ultrasonic-assisted electrodeposition which promotes the electrodeposition in the blind holes of Nd-Fe-B matrix. The corrosion resistance of Cu-coated Nd-Fe-B materials with the same coating thickness is improved gradually with increasing the ultrasonic frequency.

Key words: sintered Nd-Fe-B; ultrasonic-assisted; nanocrystalline Cu; cyanide-free electrodeposition; corrosion resistance

Sintered Nd-Fe-B magnets are used in advanced motors due to their excellent magnetic properties. However, the poor corrosion resistance due to the blind holes and Nd-rich intergranular phases restricts their application under harsh environments[1]. Currently, two major methods for corrosion resistance enhancement of Nd-Fe-B magnets are alloying (addition of Mg, Al, Co, etc.)[2] and coating (surface modification)[3-5]. Electroplated coatings are suitable for magnets because of their simplicity and effectiveness. The Ni layer obtained from an acidic bath is widely used as the coating in industrial production in recent years. However, the porous and activated Nd-Fe-B substrates are susceptible to chemical corrosion in acidic medium. Particularly, due to the low permissible cathodic current density and low deep plating ability of the nickel plating, it is difficult to deposit metal in the blind pores of the sintered Nd-Fe-B magnets. The plating solution may corrode the matrix through the holes in the meantime, resulting in a worse Nd-Fe-B magnet[3]. Nickel plating can also lead to the reduction of magnetic properties due to the magnetic shielding. Efforts have been made to solve these problems, such as using the alkaline plating solution to slow down the chemical corrosion, achieving a rapid deposition and dense coating through the maximum cathodic current density, and improving the covering power to achieve the metal deposition in the blind holes. The coatings of copper, nickel, or zinc all provide cathodic protection for the Nd-Fe-B matrix, but the corrosive elements in the environment can still infiltrate into the Nd-Fe-B matrix through the pores in the coating, which can be solved by increasing the coating thickness. However, the thicker non-magnetic coating may affect the magnetic properties of the Nd-Fe-B magnets. The ideal method should enhance the

Received date: March 14, 2021
Foundation item: Sponsored by State Key Laboratory of Rare Earth Permanent Magnetic Materials (SKLREPM17OF06); National Natural Science Foundation of China (51871201); Key R&D Project of Zhejiang Provincial Department of Science and Technology (2021C01172)
Corresponding author: Zheng Jingwu, Ph. D., Assistant Researcher, Research Center of Magnetic and Electronic Materials, College of Materials Science and Engineering, Zhejiang University of Technology, Hangzhou 310014, P. R. China, Tel: 0086-571-88320142, E-mail: zhengjw@zjut.edu.cn

compactness of the protective coatings without increasing the thickness, and thus the nanocrystalline coatings are proposed[6-8]. The Cu coatings are electrodeposited on the iron substrates using the alkaline cyanide-free solutions. Due to the high activation energy for the reduction of Cu ion caused by the coordination effect in alkaline cyanide-free bath, the maximum cathodic current density is generally less than 2 $A \cdot dm^{-2}$ [9]. Therefore, it is difficult to deposit in deep holes due to the low deposition speed and poor deep plating capacity of the traditional agitation methods. Besides, the interfacial adhesion between the coating and the substrate is weak. Tudela et al[10] found that the cathodic current efficiency can reach 90% at a current density of 4 $A \cdot dm^{-2}$ by ultrasonic-assisted electrodeposition. The obtained Ni coating has fine grains and improves the microhardness by the nanocrystalline structure[11]. Vasuoevan et al[12] demonstrated that the ultrasonic vibration can improve the limiting current density, anodic and cathodic current efficiencies, and the microhardness of the coatings. Martins et al[13] proposed that the ultrasonic-assisted electro-deposition can form a compact Cu coating with ordered structure. The filling capacity of Cu coating for the blind holes is particularly improved with the through-silicon-via (TSV) filling. Wang et al[14] reported that the filling quality of Cu electroplating is improved by 23% under the ultrasonic wave, compared with that under the normal conditions at the same current density. Chen et al[15] also showed that the blind holes with a small aspect ratio can be filled by ultrasonic agitation.

The reduction process of metal ions in the electrolyte containing coordination agent is very complex, and the high-quality coating and high current efficiency at high current density are difficult to achieve. Therefore, the electroplating system for ultrasonic-assisted electrodeposition containing coordination agent is rarely investigated. The higher current densities can increase the deposition rate to achieve the electrodeposition for blind holes, and yield more compact nanocrystalline coatings. In this research, the effects of ultrasonic frequency on the maximum current densities, surface morphology, and grain size of the coatings were investigated in the alkaline cyanide-free Cu-electro-plating baths with 1-hydroxyethylene-1, 1-diphosphonic acid (HEDPA) and triethanolamine (TEA) as the complex agents.

1 Experiment

The commercial sintered Nd-Fe-B magnets were cut into cylinders of Φ8 mm×5 mm. The specimens were treated by alkaline degreasing→water rinsing→soaking in 5vol% HNO_3 for 1 min→ultrasonic cleaning→Cu electrodeposition. The cyanide-free electrolytic solution used for electrodeposition consisted of 0.16 mol/L $CuSO_4$, 0.48 mol/L HEDPA, and 0.114 mol/L TEA[16]. All the experiments were conducted at room temperature and all the reagents were of analytical grade. The solutions were prepared with double-distilled water and the pH value was adjusted to 9.2 using 1.0 mol/L NaOH. The electrodeposited anode was electrolytic Cu placed in a bath at 25 °C.

The plating bath composed of plexiglass plate of 1.5 mm in thickness was a cuboid with the size of 150 mm×100 mm×70 mm. The anode Cu sheet was placed at both ends of the plating bath, and the plated specimen was placed in the middle of the plating bath. The plating bath and three-electrode system were both suspended above a water-filled high-power CNC ultrasonic cleaner (KQ-600KDE) with the distance of about 1 mm. The ultrasonic frequency was 0, 16, 24, 32, and 40 kHz. The microhardness of the Cu coating was measured by a microhardness tester (HVT-1000) under the loading of 4.9 N and the dwell time to 10 s. X-ray diffraction (XRD, Thermo ARL SCINTAG X'TRA X) analysis of the specimens was conducted using Cu Kα radiation (35 kV, 45 mA). The surface and cross-section morphologies of the coated specimens were observed by a Hitachi S-4700 field emission scanning electron microscope (SEM). The Hull-cell test was conducted under the condition of applied current of 3 A and electrodeposition time of 60 s. The magnetic properties of the Nd-Fe-B magnets were measured with a hysteresis loop tracer of NIM-2000.

The corrosion resistance was analyzed via the potentiodynamic polarization curves and electrochemical impedance spectroscopy (EIS). The three-electrode system was used for the electrochemical measurement with a Vertex electrochemical workstation (Ivium Technologies B.V. Holland). The coated specimens was the working electrode, the saturated calomel electrode (SCE) was regarded as the reference, and a platinum plate was the counter electrode. Measurements were conducted in the 5wt% NaCl solution at room temperature. The solution was treated by N_2 purging for 3 min before tests. EIS measurements were performed at the open circuit potentials with the alternating current (AC) perturbation of 10 mV in the frequency of 0.01 Hz~100 kHz. The polarization curves were obtained at a scan rate of 3 $mV \cdot s^{-1}$.

2 Results and Discussion

2.1 Ultrasonic effect on characteristics of Cu coating

Fig. 1 shows SEM surface morphologies of the coated Nd-Fe-B magnets under different ultrasonic frequencies. According to the potential activation theory[17], in order to improve the bonding strength between the substrate and the coating, the surface of Nd-Fe-B matrix should be activated instantaneously in the initial stage of electrodeposition. Thus, the high overpotential should be applied through the high cathodic current density, which also improves the deposition rate of the coating. Based on the effective current density range of HEDPA-TEA system, the cathodic current density of 2.0 $A \cdot dm^{-2}$ without ultrasonic effect and that of 4.0 $A \cdot dm^{-2}$ with ultrasonic effect were used. The surface morphology of deposited Cu coating without the ultrasonic is loose and porous, whereas that with the ultrasonic is dense and flat, which indicates that the ultrasonic can increase the effective cathodic current density and promote crystallization refinement. Fig. 2 shows XRD patterns of the deposited Cu coatings under different ultrasonic frequencies. The average crystallite sizes were estimated by XRD peak width of the

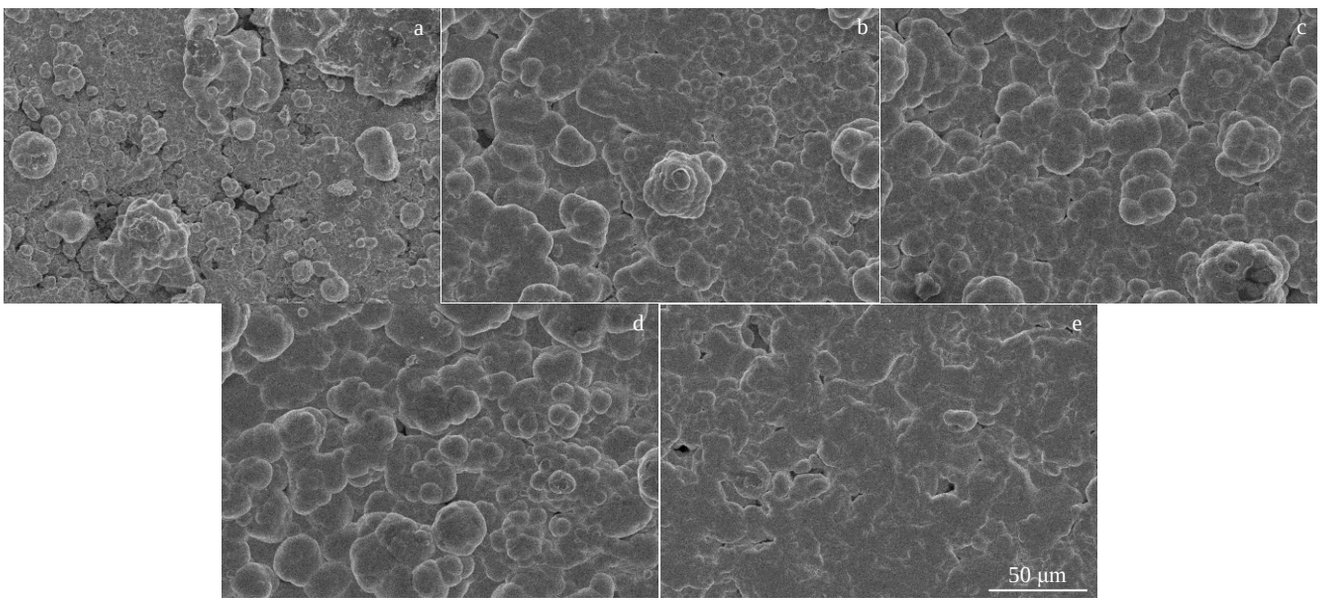

Fig.1 SEM surface morphologies of Cu-coated Nd-Fe-B magnets under different frequencies: (a) 0 Hz, (b) 16 kHz, (c) 24 kHz, (d) 32 kHz, and (e) 40 kHz

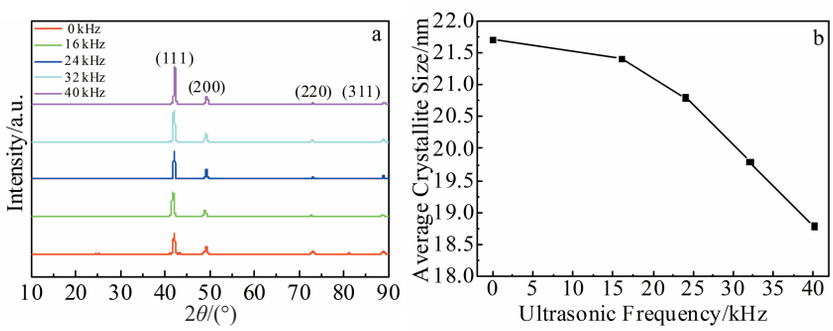

Fig.2 XRD patterns (a) and average crystallite sizes (b) of deposited Cu coating under different ultrasonic frequencies

(111) plane and Scherrer's equation, as shown in Fig.2b. With increasing the ultrasonic frequency, the average crystallite size of Cu is decreased. The crystallite size reaches 18.8 nm for the Cu coating under ultrasonic frequency of 40 kHz. The microhardness of the coatings is increased with increasing the ultrasonic frequency, as shown in Fig. 3a. Particularly, a significant increase in microhardness can be observed when the ultrasonic frequency exceeds 24 kHz. Furthermore, there is a specific relationship between the microhardness and the average crystallite size, as shown in Fig. 3b, which obeys the Hall-Petch relation[18]. The increase in microhardness is mainly attributed to the grain boundary hardening effect after grain refinement[19]. Thus, it is confirmed that the ultrasonic-assisted electroplating can refine the coating grains under the same current density due to the continuous attack towards the coating surface under ultrasonic cavitation. Besides, the grain refinement by ultrasonic can increase the crystal nucleus sites[20], therefore achieving a compact, uniform, and well-bonded coating[21].

The improvement in corrosion resistance of the Nd-Fe-B magnets mainly depends on the thickness and density of the deposited coatings. However, thicker coating results in reduced magnetic properties, especially for the nickel coating[22]. Therefore, a thin and compact Cu coating is very necessary for enhancement of the corrosion resistance of the sintered Nd-Fe-B magnets. The ultrasonic has a strong influence on the interfacial adhesion between the coating and matrix. Fig.4 shows the back-scattered electron (BSE) images of the cross-section morphologies of Cu-coated Nd-Fe-B magnets under different ultrasonic frequencies. As shown in Fig. 4, the interface between the Nd-Fe-B matrix and the coating obtained without ultrasonic effect is loose, whereas that with ultrasonic effect shows good bonding with the Nd-Fe-B matrix. The initial surface morphology of matrix has an important influence on the adhesion of the coating during electrodeposition[17]. Fig. 5 shows the surface morphologies of Nd-Fe-B matrix after electrodeposition with and without ultrasonic for 5 s. As shown in Fig. 5a, many particles are dispersed on the matrix surface, showing a weak bonding force between these particles and the matrix. As shown in

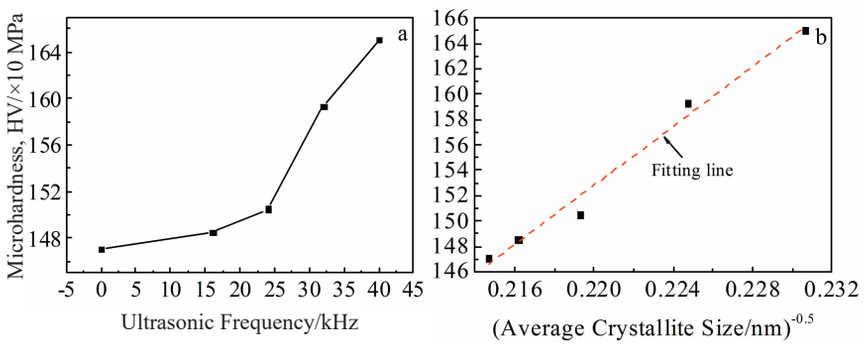

Fig.3 Microhardness of deposited Cu coating under different ultrasonic frequencies (a); relationship between microhardness and average crystallite size (b)

Fig. 5b, Cu is deposited at the grain boundaries or pits on the Nd-Fe-B matrix surface, which is attributed to the micro-jet generated by the ultrasonic cavitation effect scouring the pollutants attached to the magnet surface at the initial stage of electrodeposition. The scoured surface of Nd-Fe-B matrix is at a highly activated state before Cu deposition, which results in the high-quality coating with a close-packed layer during the initial electrodepositing stage and advanced adhesion between the coating and Nd-Fe-B matrix.

2.2 Effect of ultrasonic on electrodeposition process

Numerous blind pores are produced on the Nd-Fe-B matrix surface during the powder pressing and the sintering processes. Thus the improved filling capacity and deposition rate of Cu electroplating are required.

The electrodeposition of the blind holes in Nd-Fe-B matrix under ultrasonic was simulated using a hollow stainless steel tube with the inner diameter of 1 mm and length of 100 mm. The outer wall of the tube was shielded with the insulating tape and the tube was sealed at one end. The tube was placed horizontally in the electroplating solution with the open end facing the Cu anode. The depths of Cu electrodeposition inside the tube under different ultrasonic frequencies were measured. The longitudinal-section images of the tube are shown in Fig. 6 (the red area indicates the Cu electroplating region).

The electrodeposition depth of the tube under the ultrasonic of 40 kHz is about 7 times larger than that under mechanical agitation. The electrodeposition depth in the blind hole is increased with increasing the ultrasonic frequency, which is related to the ultrasonic cavitation. The water pressure produced by the cavitation effect causes the bubble to enter the blind holes, and thus the electroplating solution fills the pipe, which consequently expands the effective cathode current density. Therefore, the covering power is improved, and the metal is electroplated on the blind hole surface, leading to improved corrosion resistance.

Fig. 7 shows the electrodeposition distributions of Cu

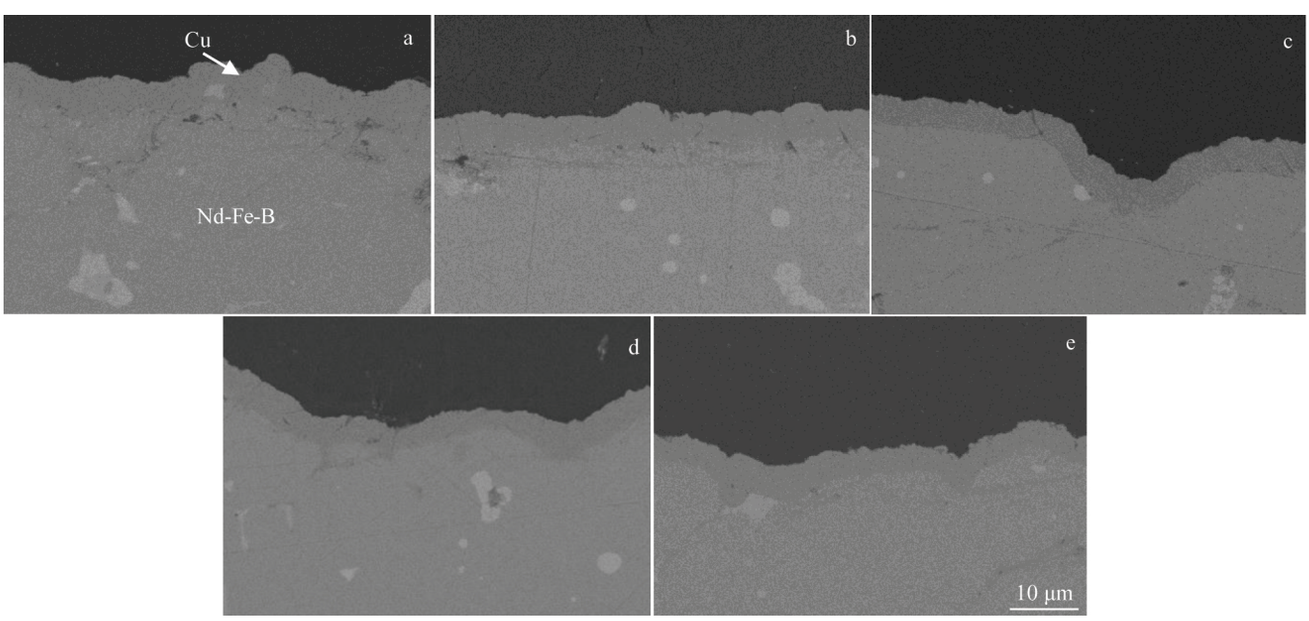

Fig.4 BSE images of cross-section morphologies of Cu-coated Nd-Fe-B magnets under different ultrasonic frequencies: (a) 0 Hz, (b) 16 kHz, (c) 24 kHz, (d) 32 kHz, and (e) 40 kHz

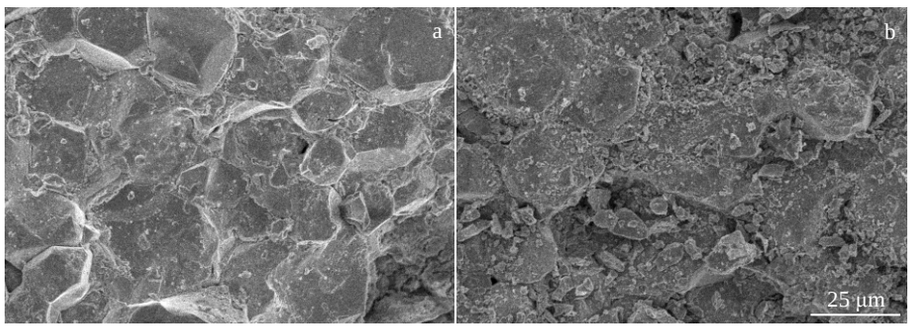

Fig.5 SEM images of Nd-Fe-B magnets after electrodeposition without ultrasonic (a) and with the ultrasonic of 40 kHz in frequency (b) for 5 s

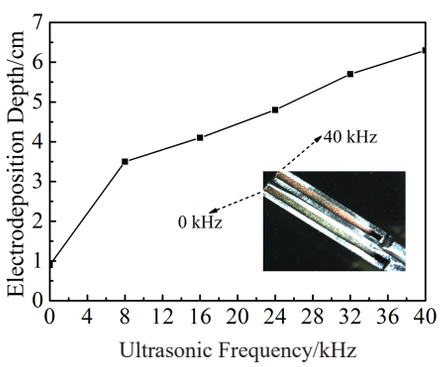

Fig.6 Electrodeposition depths for blind holes in Nd-Fe-B magnets under different ultrasonic frequencies

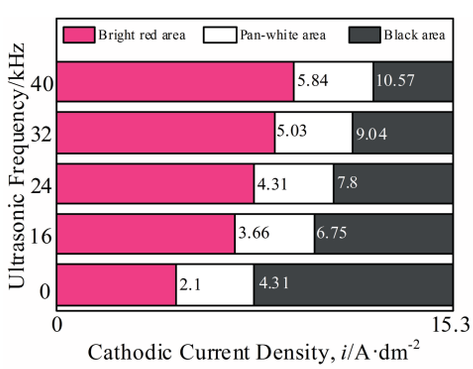

Fig.7 Electrodeposition distributions of Cu coating on Nd-Fe-B matrix under different cathodic current densities and ultrasonic frequencies in Hull-cell tests

coatings under different cathodic current densities and ultrasonic frequencies in the Hull-cell tests under a total current of 3 A. It can be found that the Cu electrodeposition mainly shows three states under the current density condition of 0~15.3 A·dm^{-2}: the bright red area with excellent quality, the pan-white area of ultra-thin coating, and the black area with the burnt deposits. The bright red area is increased with increasing the ultrasonic frequency, indicating that the efficient current density and maximum cathodic current density are increased with increasing the ultrasonic frequency. The maximum current density increases from 2.1 A·dm^{-2} (0 Hz) to 5.84 A·dm^{-2} (40 kHz), which is attributed to the decreased thickness of the diffusion layer at the electrode surface. The electrolyte scouring by ultrasonic results in a thinner area of the diffusion layer. According to the limiting current density $D_L=nFKC_i^0/\delta$ (δ is the thickness of diffusion layer, n is the transferred electron number, F is the Faraday constant, K is the electron-transfer rate constant, and C_i^0 is the bulk concentration of Cu^{2+}), D_L mainly depends on the thickness of the diffusion layer δ. The thickness declines under high-speed micro-jet agitation by ultrasonic cavitation, resulting in an increase in D_L[23]. Therefore, the higher maximum current density not only leads to a faster Cu electrodeposition rate on the Nd-Fe-B matrix surface, but also increases the nucleation rate for more crystal nucleation and better grain refinement effect[20].

Ultrasonic agitation also improves the cathodic current efficiency, as shown in Fig.8. Under the same current density of 4.0 A·dm^{-2} and the same electrodeposition duration of 5 min, the current efficiency without ultrasonic assistance is 69.38%, while it is increased to 76.3% under the ultrasonic of 16 kHz and is further increased to 92.75% under the ultrasonic of 40 kHz, because of the decrease in the overpotential of the electrode under ultrasonic vibrations[24]. In addition, the ultrasonic vibration inhibits the hydrogen evolution reaction and prevents more hydrogen atoms from adsorbing on the Nd-Fe-B matrix surface, thus reducing the potential hydrogen embrittlement of the sintered Nd-Fe-B magnets.

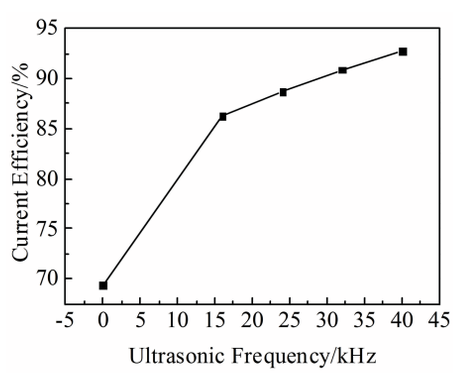

Fig.8 Current efficiency of Cu electrodeposition on Nd-Fe-B matrix under different ultrasonic frequencies

To further investigate the effect of ultrasonic on the coating electrodeposition, the cathodic polarization curves with the sintered Nd-Fe-B magnets as the working electrode under different ultrasonic frequencies were analyzed and the results are shown in Fig.9. The initial potential of Cu reduction shifts positively with the ultrasonic. Moreover, with increasing the ultrasonic frequency, the Cu electrodeposition current is increased gradually under the same reduction potential.

2.3 Effect of ultrasonic on corrosion resistance

The corrosion resistance of the sintered Nd-Fe-B magnets with deposited Cu coating was tested through the anodic polarization and AC impedance tests in 5wt% NaCl solution, and the results are shown in Fig. 10. The polarization curve was analyzed by the Tafel zone extrapolation method, as shown Fig. 10a. The corrosion potential (E_{corr}), corrosion current density (i_{corr}), and other parameters can be obtained, as listed in Table 1. It can be seen that with increasing the ultrasonic frequency, the corrosion potential of the coating is increased, while the corrosion current density is gradually decreased. The corrosion resistance of the coating under ultrasonic electrodeposition is much better than that under mechanical agitation. Fig. 10b shows EIS Nyquist plots of Cu electrodeposition at 0.1 V vs. SCE under different ultrasonic frequencies. The impedance curve in the high-frequency region for the Nd-Fe-B matrix with a Cu coating of 3 μm in thickness shows a semicircular capacitance arc. With increasing the ultrasonic frequency, the capacitance radius is increased, suggesting the improved corrosion resistance. According to the fourth quadrant of the Nyquist diagram of the Cu coating under ultrasonic, the semicircle representing the inductance characteristic appears in the low-frequency region, and the radius of the semicircle is slightly increased with increasing the ultrasonic frequency. The inductive reactance phenomenon can be attributed to the formation of the passive film on the electrode surface during the corrosion process of Cu coating[25].

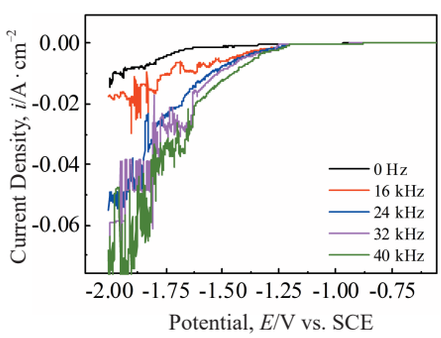

Fig.9 Cathodic polarization curves of Cu electrodeposition on Nd-Fe-B matrix under different ultrasonic frequencies

According to the characteristics of the impedance spectrum, the equivalent circuits are shown in Fig. 11. R_s is the solution resistance, R_{ct} is the charge transfer resistance, R_p is the pore resistance of coating, R_c is the film resistance, W is the warburg impedance, L is the inductance, CPE is the constant phase element representing the film capacitance, and n is the charge transfer efficiency. The analysis results are listed in Table 1. With increasing the ultrasonic frequency, R_c of the

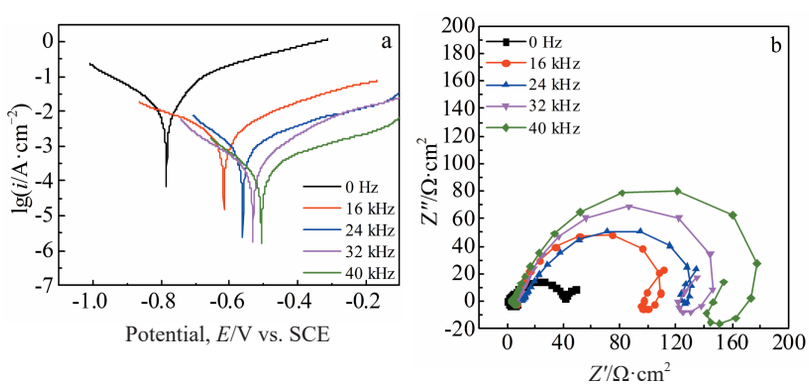

Fig.10 Potentiodynamic polarization curves (a) and Nyquist plots (b) of Cu-coated Nd-Fe-B magnets in 5wt% NaCl solution under different ultrasonic frequencies

Table 1 Electrochemical parameters from polarization curves and fitting parameters of EIS of Cu-coated Nd-Fe-B magnets under different ultrasonic frequencies

Frequency/kHz	Electrochemical parameter		Circuit simulation parameter					
	E_{corr}/V vs. SCE	i_{corr}/A·cm^{-2}	CPE/F·cm^{-2}	R_{ct}/Ω·cm^2	R_p/Ω·cm^2	R_c/Ω·cm^2	L/H·cm^2	n
0	−0.7849	0.0586	0.000 740	-	-	38.10	-	0.8097
16	−0.6171	0.0254	0.001 000	277.0	128.0	87.54	58.1	0.8207
24	−0.5612	0.0162	0.001 990	172.0	242.0	100.54	60.4	0.6924
32	−0.5313	0.0112	0.001 358	182.0	272.7	109.15	76.4	0.7359
40	−0.5059	0.0089	0.000 935	296.8	219.8	126.21	257.5	0.8124

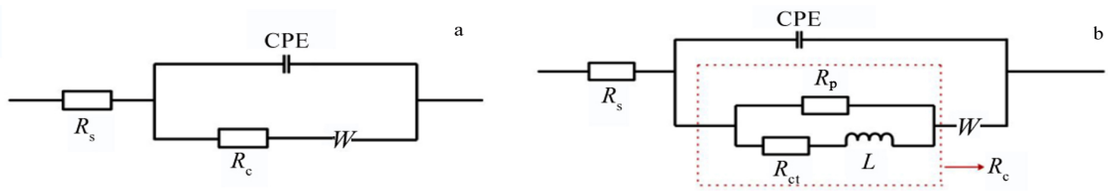

Fig.11 Equivalent circuits for EIS data of Cu-coated Nd-Fe-B magnets without (a) and with (b) ultrasonic

Table 2 Magnetic properties of Cu-coated Nd-Fe-B magnets under different ultrasonic frequencies (Cu coating thickness of 3 μm)

Ultrasonic frequency/kHz	0	16	24	32	40
Remnant magnetic induction intensity, B_r/T	1.22	1.19	1.21	1.22	1.21
Intrinsic coercivity, H_{cj}/kA·m^{-1}	1950.76	1922.10	1940.25	1923.06	1928.07
Maximum magnetic energy product, BH_m/kJ·m^{-3}	266.77	265.14	262.51	264.65	265.31

Cu-coated Nd-Fe-B matrix is gradually increased. The modeling further supports the fact that the coatings obtained by ultrasonic electrodeposition have a better protective performance on the sintered Nd-Fe-B matrix than those by the mechanical agitation.

Both the anodic polarization curve and the impedance curve show the advanced corrosion resistance of the Cu coating on the sintered Nd-Fe-B matrix by ultrasonic-assisted electrodeposition, which is attributed to the grain refinement of the Cu electroplating layer and the formation of the nanocrystalline structure. Compared with the crystallite, the nanocrystal has a larger specific surface area for a quicker corrosion to form a dense passivated film in some alkaline environments[26], resulting in stronger corrosion resistance of the Cu coating. In addition, due to the grain refinement, the porosity of the coating is smaller, thereby greatly reducing the possibility of the corrosive solution entering the Nd-Fe-B matrix through the coating pores, which is important for the dense cathodic coating in the surface protection for the highly active sintered anodic Nd-Fe-B magnets.

2.4 Ultrasonic effect on magnetic properties

The magnetic properties of the Cu-coated sintered Nd-Fe-B magnets under different ultrasonic frequencies are investigated, as listed in Table 2. It can be seen that the ultrasonic frequency has little effect on the magnetic properties of the sintered Nd-Fe-B magnets.

3 Conclusions

1) With increasing the ultrasonic frequency, the maximum effective current density and efficiency of Cu electrodeposition are improved. The cathodic current efficiency reaches 92.75% at the current density of 4.0 A·dm^{-2} under the ultrasonic frequency of 40 kHz.

2) The Cu coating of the sintered Nd-Fe-B magnets can be electrodeposited quickly to decrease the chemical corrosion in the electrodeposition bath under the ultrasonic assistance. With increasing the ultrasonic frequency, the corrosion resistance of the Cu-coated sintered Nd-Fe-B magnets is gradually improved.

3) The Cu coating grains are refined and the microhardness of Cu coating is increased. The deposited surfaces are smooth and dense. The average crystallite size of 18.8 nm is obtained for the Cu coating at the cathode current density of 4.0 A·dm^{-2} under the ultrasonic frequency of 40 kHz.

4) The ultrasonic-assisted electrodeposition method can increase the covering power, promote the electrodeposition in the blind holes, and improve the adhesion between the Cu coating and the sintered Nd-Fe-B magnet matrix. Ultrasonic has little impact on the magnetic performance of the Cu-coated sintered Nd-Fe-B magnet .

References

1 Isotahdon E, Huttunen-Saarivirta E, Kuokkala V T *et al*. *Materials Chemistry and Physics*[J], 2012, 135(2-3): 762

2 El-Azizv A M. *Materials and Corrosion* [J], 2003, 54(2): 88

3 Zheng Jingwu, Chen Haibo, Qiao Liang *et al*. *Journal of Magnetism and Magnetic Materials*[J], 2014, 371: 1

4 Cao R, Zhu L Q, Liu H C *et al*. *Surface and Coatings Technology* [J], 2017, 309: 820

5 He W T, Zhu L Q, Chen H N *et al*. *Applied Surface Science*[J], 2013, 279: 416

6 Kaseem M, Choi K, Ko Y G. *Materials Letters*[J], 2017, 196: 316

7 Zhou Xiaowei, Liu Zhenguang, Wang Yuxin *et al*. *Rare Metal Materials and Engineering*[J], 2019, 48(12): 3978

8 Dong Nan, Zhang Caili, Li Juan *et al*. *Rare Metal Materials and Engineering*[J], 2016, 45(4): 885

9 Zheng Jingwu, Chen Haibo, Cai Wei *et al*. *Materials Science and Engineering B*[J], 2017, 224: 18

10 Tudela I, Zhang Y, Pal M *et al*. *Surface and Coatings Technology* [J], 2015, 264: 49

11 Xia F F, Liu C, Wang F *et al*. *Journal of Alloys and Compounds* [J], 2010, 490(1-2): 431

12 Vasuoevan R, Devanathan R, Chidambaram K G. *Metal Finishing*[J], 1992, 90(10): 23

13 Martins L, Martins J I, Romeira A S *et al*. *Materials Science Forum*[J], 2004, 455-456: 844

14 Wang Fuliang, Zeng Peng, Wang Yan *et al*. *Microelectronic Engineering*[J], 2017, 180: 30
15 Chen Q W, Wang Z Y, Cai J *et al*. *Microelectronic Engineering* [J], 2010, 87(3): 527
16 Zheng Jingwu, Chen Haibo, Cai Wei *et al*. *Journal of the Electrochemical Society*[J], 2017, 164(12): 798
17 Feng Shaobin, Shang Shibo, Bao Xiang *et al*. *Acta Physico-Chimica Sinica*[J], 2005, 21(5): 463 (in Chinese)
18 Zhang P, Li S X, Zhang Z F. *Materials Science and Engineering A*[J], 2011, 529: 62
19 Sriraman K R, Raman S G S, Seshadri S K. *Materials Letters*[J], 2007, 61(3): 715
20 Zhou Xiaowei, Shen Yifu. *Applied Surface Science*[J], 2015, 324: 677
21 Mallik A, Ray B C. *Thin Solid Films*[J], 2009, 517(24): 6612
22 Alamgir A K M, Gu C, Han Z. *Physica C: Superconductivity*[J], 2006, 440(1-2): 35
23 Leigh C, Hagenson L, Doraiswamy K. *Chemical Engineering Science*[J], 1998, 53(1): 131
24 Chang J H, Ellis A V, Yan C T *et al*. *Separation and Purification Technology*[J], 2009, 68(2): 216
25 Quentin M, Zhao C. *Journal of Power Sources*[J], 2021, 488: 229 245
26 Wang Liping, Zhang Junyan, Gao Yan *et al*. *Scripta Materialia* [J], 2006, 55(7): 657

无氰电镀液中超声电沉积耐腐蚀纳米晶铜镀层

郑精武[1]，陈意顺[1]，付永成[1,3]，张　栓[1]，乔　梁[1]，蔡　伟[1]，唐谊平[1]，衣晓飞[2]，陈静武[2]，李旺昌[1]，
应　耀[1]，余　靓[1]，刘友好[2]，黄秀莲[2]，车声雷[1]

(1. 浙江工业大学 材料科学与工程学院 磁电材料研究所，浙江 杭州 310014)
(2. 大地熊新材料股份有限公司 稀土永磁材料国家重点实验室，安徽 合肥 231500)
(3. 中科芯集成电路有限公司，江苏 无锡 214072)

摘　要：通过超声辅助电沉积法，在无氰络合电镀液中以高阴极电流密度在钕铁硼磁体上电沉积获得纳米晶铜防护镀层，研究了不同超声波频率下的镀层形貌、晶粒尺寸、显微硬度和耐腐蚀性能。结果表明，随着超声波频率的增加，络合电镀液体系的铜电沉积有效阴极电流密度显著增加，相应的阴极电流效率也提高，从而获得致密的纳米晶铜镀层。在阴极电流密度为4.0 A·dm^{-2}和超声波频率为40 kHz的条件下，能够获得平均晶粒尺寸为18.8 nm的铜镀层。超声辅助电沉积法还能促进烧结钕铁硼基体盲孔内的铜沉积，从而改善基体与镀层之间的结合力。在同样的镀层厚度下，烧结钕铁硼表面所沉积镀层的耐腐蚀性随超声波频率的提高而优化。

关键词：烧结钕铁硼；超声辅助；纳米晶铜；无氰电沉积；耐腐蚀性能

作者简介：郑精武，男，1975年生，博士，副研究员，浙江工业大学材料科学与工程学院磁电材料研究所，浙江 杭州 310014，电话：0571-88320142，E-mail：zhengjw@zjut.edu.cn